Lawrence Berkeley National Laboratory

Title:
Aqueous and gaseous nitrogen losses induced by fertilizer application

Author:
Gu, C.

Publication Date:
04-09-2009

Publication Info:
Lawrence Berkeley National Laboratory

Permalink:
http://www.escholarship.org/uc/item/1p49x2bj

Citation:
Gu, C.(2009). Aqueous and gaseous nitrogen losses induced by fertilizer application . Lawrence Berkeley National Laboratory: Lawrence Berkeley National Laboratory. LBNL Paper LBNL-1689E. Retrieved from: http://www.escholarship.org/uc/item/1p49x2bj

eScholarship
University of California

eScholarship provides open access, scholarly publishing services to the University of California and delivers a dynamic research platform to scholars worldwide.

Aqueous and Gaseous Nitrogen Losses Induced by Fertilizer Application

Chuanhui Gu[1], F. Maggi,[1] W.J. Riley[2], R.T. Venterea[3], G.M. Hornberger[4], T. Xu[2], N. Spycher[2], C. Steefel[2], N.L. Miller[1,2], C.M. Oldenburg[2]

[1]Berkeley Water Center, University of California, Berkeley, CA; [2]Lawrence Berkeley National Laboratory, Berkeley, CA; [3]USDA-ARS, Soil and Water Management Unit, St. Paul, MN; [4]Vanderbilt University, Nashville, TN

[1] Berkeley Water Center, Department of Civil and Environmental Engineering, 413 O'Brien Hall, University of California, Berkeley, Berkeley, CA, 94720
[2] Earth Science Division, Lawrence Berkeley National Laboratory, Berkeley, CA, 94720
[3] Soil and Water Research Management Unit, USDA Agricultural Research Service, St.Paul, MN, 55108
[4] Department of Environmental Sciences, University of Virginia, P.O.Box 400123, Charlottesville, VA, 22904-4123

Abstract

In recent years concern has grown over the contribution of nitrogen (N) fertilizer use to nitrate (NO_3^-) water pollution and nitrous oxide (N_2O), nitric oxide (NO), and ammonia (NH_3) atmospheric pollution. Characterizing soil N effluxes is essential in developing a strategy to mitigate N leaching and emissions to the atmosphere. In this paper, a previously described and tested mechanistic N cycle model (TOUGHREACT-N) was successfully tested against additional observations of soil pH and N_2O emissions after fertilization and irrigation, and before plant emergence. We used TOUGHREACT-N to explain the significantly different N gas emissions and nitrate leaching rates resulting from the different N fertilizer types, application methods, and soil properties. The N_2O emissions from NH_4^+-N fertilizer were higher than from urea and NO_3^--N fertilizers in coarse-textured soils. This difference increased with decreases in fertilization application rate and increases in soil buffering capacity. In contrast to methods used to estimate global terrestrial gas emissions, we found strongly non-linear N_2O emissions as a function of fertilizer application rate and soil calcite content. Speciation of predicted gas N flux into N_2O and N_2 depended on pH, fertilizer form, and soil properties. Our results highlighted the need to derive emission and leaching factors that account for fertilizer type, application method, and soil properties.

1 Introduction

Anthropogenic input of reactive nitrogen to ecosystems has led to significant environmental consequences [Galloway et al., 2003; Aber et al, 2003]. Use of nitrogen fertilizers in agriculture has a direct impact on water (NO_3^-) and atmospheric pollution

(N_2O, NO, NH_3) [Vitousek et al. 1997]. Groundwater NO_3^- concentrations exceed drinking-water standards in many areas [*Byrnes*, 1990; *Scanlon et al.*, 2007], resulting in potential human health effects (i.e., methemoglobulinemia [*Hill*, 1996]). Elevated NO_3^- concentrations in leachate and surface water can also lead to eutrophication of lakes and estuaries [*Lowrance et al.*, 1997]. Agricultural land also has been identified as the major anthropogenic source of nitrous oxide (N_2O) [*Mosier et al.*, 1998; IPCC 2007] and an important source of nitric oxide (NO) [*Yienger and Levy*, 1995] entering the atmosphere. Because the formation of these N species in soils is primarily through volatilization, nitrification, and denitrification [*Bremner*, 1997; *McKenney and Drury*, 1997; Firestone and Davidson 1989], their release rates can drastically increase with elevated inputs of nitrogen from fertilization. Nitrous oxide (N_2O) is an important greenhouse gas and is also involved in the destruction of stratospheric ozone [*IPCC*, 2001]. Nitric oxide (NO) emissions contribute to the formation of tropospheric ozone and acid deposition [*McTaggart et al.*, 2002]. NH_3 emissions affect the environment in the form of wet and dry deposition of NH_4^+ salts, causing acidification of poorly buffered soils and eutrophication [*vanderWeerden and Jarvis*, 1997]. Such concerns have stimulated extensive studies in recent years to identify potential mitigation options for reducing N leaching and emission from agro-ecosystems [*Skiba et al.*, 1997].

Several forms of N fertilizer are currently in use, resulting in different N substrates (i.e., NH_4^+, NO_3^-) for these loss pathways [*Davidson et al.*, 1991] and plant uptake. Ammonium undergoes nitrification under aerobic conditions, while nitrate is reduced by denitrification under anaerobic conditions [*Conrad*, 1996]. There is strong evidence of a connection between the magnitude of emissions and the type of N fertilizer

applied [*Clayton et al.*, 1997; *Eichner*, 1990]; and also for a link between NO_3^- leaching and fertilizer type [*Jiao et al.*, 2004].

Understanding the effect of fertilizer type on N losses in agricultural fields is essential for developing a strategy to mitigate gaseous and aqueous losses. Although both field and laboratory measurements have been made to examine how fertilizer type affects N loss, analysis of the plethora of factors involved in the coupled N cycle requires a mechanistic modeling framework to generalize and extend the empirical work.

There are a number of published models simulating soil water dynamics and N turnover (e.g., RZWQM [Ahuja et al., 2000], DAYCENT [Parton et al, 2001], GLEAMS [Leonard et al, 1987], BIOME-BGC [Running and Gower, 1994; Thornton et al, 2005], PnET-BGC [Gbondo-Tugbawa et al. 2001], DNDC [Li et al., 1992]). All these models consider soil inputs and outputs and simulate N cycle processes with varying degrees of complexity. Few existing models, however, are capable of accurately capturing the observed effects of different fertilizer types on nitrogen losses (e.g., [*Frolking et al.*, 1998]). Typically , processes such as nitrification and denitrification have been represented in models as functions of substrate and available carbon that are modified by dimensionless factors for soil water content and temperature [*Li et al.*, 1992; *Parton et al.*, 1996]. Such simple models have limitations, however, particularly for examining variability at fine temporal and spatial scales. For example, short-term temporal variations in N emission and leaching are too large to be explained from simple functions of soil water content, temperature, or N and C substrates [*Blackmer et al.*, 1982; *Flessa et al.*, 1995; *Hall et al.*, 1996; *Hutchinson et al.*, 1997], indicating that N-losses are additionally impacted by complex interactions among N transformation and transport

processes and concurrent environmental conditions. Such interactions need to be represented in models to simulate nitrogen fluxes reliably [*Kroeze et al.*, 2003]. The kinetics of NH_4^+ oxidation and NO_3^- reduction pathways, which have been modeled individually [*Grant et al.*, 1993; *Leffelaar and Wessel*, 1988; *Mcconnaughey and Bouldin*, 1985; *Riley and Matson*, 2000; *Venterea and Rolston*, 2000a], must be linked with transport processes [e.g., advection and diffusion] if they are to be used to estimate N losses under field conditions. This linkage is especially important during and immediately after hydrological events (e.g., irrigation, precipitation, spring thaw, etc.) when N transformation and transport are affected by water movement *[Hutchinson et al., 1993; Scanlon and Kiely, 2003]*. There are very few models that include comprehensive N transport and transformation dynamics. Some of the models, such as MIKESHE [Refsgaard and Storm, 1995] and MODFLOW-MT3D [Harbaugh et al, 2000, Zheng, et al, 2000] are transport-oriented with less mechanistic treatment of N biogeochemical processes; and some, such as DAYCENT [Parton, et al., 2001] and SOILN[Li et al., 1992], have N turnover functions but with more limited transport features.

The goal of the work presented here was to merge representations of relevant N cycle processes and thereby improve model accuracy. Our previous paper [Maggi et al., 2008] described in detail the mechanistic N model TOUGHREACT-N, which implements N biogeochemical processes into the fully distributed (three dimensional) subsurface water flow and reactive transport model TOUGHREACT (Xu et al, 1998). Here we present some update developments to TOUGHREACT-N. The updated model includes comprehensive ion chemistry capable of simulating the application of NH_4^+/NO_3^- forming fertilizers and associated urea hydrolysis, pH dynamics, and pH

dependent NH_3 volatilization. It also simulates dissolved organic carbon (DOC) dissolution and adsorption in order to better describe carbon substrate dynamics. TOUGHREACT-N was previously applied to a field experiment in Sacramento, CA, and successfully simulated N speciation and losses following fertilization and irrigation. Here, we applied TOUGHREACT-N to a field experiment in Burgundy, France, to simulate 31-day pre-emergence N losses following multiple types of fertilizer application. Transient pulse emissions and N leaching after fertilization accounted for a large portion of N-loss [*Eichner*, 1990; *Henault et al.*, 1998]. Finally, after testing the model against observed soil moisture, pH, and N_2O fluxes, we examined the effects of different fertilizer and soil types on NO_2^- and NO_3^- leaching, and on transient NH_3, N_2O, and NO gas emissions under different fertilizer application practices and environmental conditions.

2 Materials and Methods

2.1 TOUGHREACT-N model

The multiphase flow and transport model-TOUGHREACT [*Pruess et al.*, 1999; *Xu et al.*, 2005] was taken as the basis for the implementation of an N-Cycle model (TOUGHREACT-N, [*Maggi et al.*, 2008s]). TOUGHREACT-N simulates the soil N cycle affected by climate, microbial activity, water and fertilizer inputs, and soil type by coupling multiphase advective and diffusive transport, multiple Monod kinetics, and equilibrium and kinetic geochemical reactions (Figure 1). Although TOUGHREACT has 3D flow and transport capability, here we only discuss the 1D domain for simplicity.

Soil Moisture Dynamics

The model numerically simulates variably saturated water flow using Richards' equation;

$$\frac{\partial \theta}{\partial t} = \frac{\partial}{\partial z}\left[K(\theta)\left(\frac{\partial[\psi(\theta)}{\partial z} + 1 \right)\right] \qquad (1)$$

where θ is the soils moisture, and $\psi(\theta)$ and $K(\theta)$ are the water potential and hydraulic conductivity, respectively, computed as functions of soil type according to van Genuchten (1980).

Multiphase Transport

TOUGHREACT-N simulates chemical transport using a multiphase form of the advection-dispersion-reaction equation to describe chemical advection in the aqueous phase and diffusive transport in the gas and aqueous phases. The model conceptualizes the transient mass balance of chemical species in aqueous, gaseous, and solid phases as:

$$\frac{\partial}{\partial t}(\theta_a C_a + \theta_g C_g + \rho_b C_s) = \frac{\partial}{\partial z}(\theta_a D_a \frac{\partial C_a}{\partial z} + \theta_g D_g \frac{\partial C_g}{\partial z}) - \frac{\partial(v_a C_a)}{\partial z} + S \qquad (2)$$

Where C_a, C_g and C_s are the species concentrations (mol m^{-3}) in the aqueous, gaseous and solid phases, respectively, θ_a and θ_g are the volumetric fractions (m^3 m^{-3}) of the aqueous and gaseous phase, respectively, ρ_b is the dry bulk density of the solid phase (kg m^{-3}), v_a is the volumetric flux of the aqueous phase (m s^{-1}), D_a and D_g are the effective diffusion coefficient in the liquid and gaseous phase, respectively, including effect of tortuosity (m^2 s^{-1}), S is the source/sink term (kg m^{-3} s^{-1}), t is time (s), and z is the spatial coordinate (m). A linear isotherm is used to relate species concentrations in the aqueous and solid phases, while Henry's law is used to relate species concentrations in the aqueous and gaseous phases.

Gas species diffusion coefficients are computed as a function of temperature, pressure, molecular weight, and molecular diameter. Assuming ideal gas behavior, the tracer diffusion coefficient of a gaseous species can be expressed as [Lasag, 1998]:

$$D_g = \frac{RT}{3\sqrt{2}\pi P N_A d_m^{\ 2}} \sqrt{\frac{8RT}{\pi M}} \tag{3}$$

Where D_g is the gaseous diffusion coefficient ($m^2\ s^{-1}$), R is molar gas constant, T is temperature (K), P is pressure ($kg\ m^{-1}\ s^{-2}$), N_A is Avogadro's number, d_m is molecular diameter (m), and M is molecular weight ($kg\ mol^{-1}$)

The Nitrogen Cycle

A full description of inorganic N biogeochemical processes in TOUGHREACT-N can be found in Maggi et al., [2008]. Briefly, four main N-cycle pathways (nitrification, nitrifier denitrification, denitrification, and chemo-denitrification) (Table 1) were implemented to model N-losses and their partitioning between gaseous and aqueous phases. The reaction network and transport mechanism used in TOUGHREACT-N is depicted in Figure 1.

Nitrification, Dentrification and Aerobic Respiration

Multiple-Monod microbial growth and substrate utilization kinetics are used to describe each step of nitrification, denitrification and aerobic respiration:

$$S_i = B_i \hat{\mu}_i \prod_{k=1}^{N_m} \frac{C_{i,k}}{K_{Mi,k} + C_{i,k}} \frac{K_{I\,i}}{K_{I\,i} + I_i} f(S_\theta) g(pH)\,. \tag{4}$$

Here, S_i is the reaction rate of the ith aqueous species [$mol\ m^{-3} s^{-1}$], B_i is biomass [$molm^{-3}$], $\hat{\mu}_i$ is maximum specific growth constant [s^{-1}], $C_{i,k}$ is the concentration of the kth species [$mol\ m^{-3}$], I_i is the concentration of the ith inhibitor [$mol\ m^{-3}$] (e.g. O_2), $K_{Mi,k}$ is the kth Monod half-saturation constant of the ith species, N_m is the number of Monod terms, K_{Ii} is

*i*th inhibition constant, I_i is ith inhibitor concentration, and $f(S_\theta)$ and $g(pH)$ are two piecewise linear functions accounting for microbial water and acidity stress. Finally, stoichiometric production or consumption is simulated by multiplying S_i by the corresponding stoichiometric coefficients based on reaction equations. Note that dissolved oxygen concentration is explicitly simulated based on the balance between diffusion and consumption from stoichiometric relationships. Oxygen inhibition effects on denitrification are simulated by introducing an inhibition relationship (analogous to $g(pH)$).

Microbial Dynamics

The dynamics of each microbial biomass (B_i) is assumed to satisfy the Monod equation:

$$\frac{\partial B_i}{\partial t} = \sum_c S_{ic} Y_{ic} - \delta_i B_i \tag{5}$$

with Y_{ic} the yield coefficients for B_i to grow upon the substrate c [mg mol^{-1}], S_{ic} as in Eq. (3) for each substrate c, and δ_i the biomass death rate [s^{-1}].

Chemodenitrification

Chemical decomposition of nitrite plays an important role in NO emissions from acidic soils [Venterea and Rolston 2000]. The contribution of chemical decomposition of HNO_2 into HNO_3 and NO was taken into account by the reaction:

$$3HNO_2 \rightarrow H_2O + HNO_3 + 2NO(aq)\,. \tag{6}$$

TOUGHREACT-N assumes first-order kinetics for this reaction based on the study of Venterea and Rolston [2000].

pH Dyanmics

TOUGHREACT-N simulated temporal change in soil pH by directly predicting, and consumption estimated from stoichiometric reaction equations (Table 1b&c in Maggi et al., 2008).

Dissolved Organic Carbon (DOC)

Different sizes of organic matter pools exist in the soil. In the present study we simplified the soil carbon dynamics by taking into account a single organic matter pool, Particulate Organic Carbon (POC). Give the long time scales of soil carbon turnover (from days to centuries), this simplification is not expected to affect predicted N dynamics over the monthly time scale considered in this study . Note that POC can not be used directly by microorganisms. Hydrolysis and solubilization of these compounds are necessary steps of latter microbial energy or growth use. This process may act as a source of labile DOC, which is later subject to transport processes (e.g., advection and dispersion). Based on the DOC adsorption studies of Jardine et al-[1992], a kinetic dissolution model is used to simulate the release of DOC from POC. The model has the following form

$$\frac{dPOC}{dt} = \alpha \times (k_d \times DOC - POC), \qquad (7)$$

where POC is the mass of solid organic carbon per unit mass of solids (MM^{-1} solids), α is a first-order mass transfer coefficient (1/T), K_d is a linear distribution coefficient for the layer (L^3 water/M solids), and DOC is the dissolved organic carbon concentration (ML^{-3} water).

In TOUGHREACT-N, DOC is competitively consumed by Ammonium Oxidizer Bacteria (AOB) and Denitrifier (DEN) during denitrification, and by other hetertrophic and aerobic microbes (AER) during respiration, resulting in CO_2 production (Figure 1).

Cation Exchange

Soil buffering capacity plays a central role in regulating NH_3 volatilization and soil microbial metabolism. Soil pH is buffered mainly by exchangeable base cations in both mineral and organic form. In TOUGHREACT-N, cation exchange is described as an equilibrium reaction between an exchangeable cation and an exchange site. We apply the Gaines-Thomas convention as a general expression of cation exchange reactions [*Appelo and Postma*, 1993]. The concentration of the jth exchanged cation, w_j (mol m^{-3}), is estimated from the jth equivalent fraction:

$$w_j = \beta_j CEC \rho_s z_j \frac{(1-\phi)}{100\phi}, \tag{8}$$

where β_j is the equivalent fraction, *CEC* is the cation exchange capacity (meq of cations per 100 gram of solid), ϕ is the porosity (m^3 m^{-3}), ρ_s is the density of the solids (g cm^{-3}), and z_j is the cation charge (-).

Urea Hydrolysis

TOUGHREACT-N simulates the N-cycle transformations of several widely used N fertilizers, including urea, anhydrous ammonia, ammonium, and nitrate based fertilizers. When applied to soil, urea is hydrolyzed by the ubiquitous urease enzyme, producing NH_4^+ and other inorganic C compounds whose form depends on soil pH. TOUGHREACT-N computes urea hydrolysis according to:

$$CO(NH_2)_2 + H^+ + 2H_2O \rightarrow 2NH_4^+ + HCO_3^- \tag{9}$$

TOUGHREACT-N simulates the urea hydrolysis rate (R_u, g m^{-3} s^{-1}) as a function of soil pH and moisture [*Youssef et al.*, 2005] using Michaelis-Menten kinetics.

$$R_u = f(S_\theta)g(pH)\mu_u(\frac{C_u}{K_u + C_u})(\frac{\rho}{\theta}) \quad (10)$$

where μ_u is the maximum reaction rate (s^{-1}), K_u is the half-saturation constant (g m^{-3}), and C_u is the urea-N concentration (g m^{-3}). $f(S_\theta)$ and $g(pH)$ are two piecewise linear functions accounting for microbial water and acidity stress.

2.2 Model Evaluation

For this study, we used observations from a rapeseed field on a gleyic luvisol located at Longchamp in Burgundy in eastern France from March-Apr 1997 to test TOUGHREACT-N [*Henault et al.*, 1998]. The inorganic fraction of the 0 - 20 cm layer of this soil contained 20% clay, 69% silt, and 11% sand, which falls into silt loam textural classes. The porosity of 0.46 was adapted as a typical value of silt loam for later simulation. The organic C content, organic N content, pH and bulk density in this depth interval were 1.1%, 0.09%, 6.0 ($\pm$ 0.3), and 1.40 g cm^{-3}, respectively. In the experiment, four different inorganic nitrogen fertilizers were applied in solid form: Ammonium Nitrate (NH_4NO_3); Ammonium Sulfate ($(NH_4)_2SO_4$); Urea ($CO(NH_2)_2$), and Potassium Nitrate (KNO_3) on March 3 (corresponding to time zero in our simulations) at a dose of 100 kg N ha^{-1}, and on March 18 at a dose of 70 kg N ha^{-1}. Available measurements consist of soil water content (integrated from 0 to 17 cm depth), pH (mean value of 0-20 cm depth), and N_2O fluxes by static chamber method at various times over the subsequent five months. To focus our results on the period before plant emergence, we tested the model with the first 31 days of measurements after fertilization.

2.3 Simulation Description

We selected a set of chemical species (Table 2) to represent the geochemical system in the field. Fifteen primary species were considered in determining the ion solute chemistry. Secondary species were produced by aqueous complexation, gas dissolution and exsolution, and precipitation and dissolution occurring under equilibrium and kinetically-controlled conditions.

For our numerical experiments, we used a one-dimensional vertical column 0.6 m deep divided equally into 50 layers. The column depth encompasses the dynamically active zone for N-cycle reactions in the agricultural field experiment described in Henault et al. [1998].

Initial and Boundary Conditions

Prior to simulation of fertilizer application, a model spin-up was performed to calculate initial soil water chemistry, a nearly equilibrated N free water chemistry using oversaturated CO_2 produced by microbial respiration interacting with soil buffering capacities (i.e., ion exchange and calcite). The spin-up simulation of chemical equilibrium (i.e., $CaCO_3$-H_2O-CO_2 system) was calibrated by initial soil pH of 6.0. Next, the initial conditions were assigned according to the observed initial values, or obtained from calibration with observations (Table 4). Simulations with different fertilizer types were performed by initializing the relevant N species concentrations. Surface broadcast of fertilizer was simulated by assigning fertilizer concentrations in the top soil control volume (0-1.25 cm depth) (**Table 3**).

The bottom boundary condition for water saturation was fixed at 0.45, as observed in the field. Initial water saturation was set as 0.82 between 0-10 cm and 0.8

between 10-60 cm (Table 4) by calibration with observed soil moisture. Per reported values, the irrigation flux was set as 3.5×10^{-1} m^3 H_2O m^{-2} s^{-1} for 3 hours on day 15. Partial pressures of the gaseous species at the soil surface were kept constant and equal to 0.209 bar for O_2 (g) and to 4×10^{-4} bar for CO_2 (g), and equal to zero for all other gases. Surface fluxes of NO (g), N_2O (g), N_2(g), CO_2 (g), NH_3 (g), and O_2 (g) were computed from soil-surface concentration gradients. N leaching flux was estimated as the product of aqueous concentrations at depth and the simulated water flux.

Model Calibration and Testing

A first calibration of the flow model was performed to determine optimal soil hydraulic parameters. A stepwise calibration was taken, since the simulated N transport and transformation strongly depends on the accuracy of simulated soil moisture.

Calibration was assisted by PEST [Parameter ESTimation, Papadopulos and Associates Inc.] to minimize the weighted least-square objective function between experimental and simulated data of liquid saturation using the Levenberg-Marquardt method. For calibration of biochemical parameters we used the weighted objective function between experimental and simulated data of pH and N_2O fluxes. A classical split sampling in data type test was conducted using the data set from $(NH_4)_2SO_4$ and KNO_3 treatments for model calibration and the data set from NH_4NO_3 and $CO(NH_2)_2$ treatments for model testing.

The soil was modeled as a silt loam with particle density of 2.6 g cm^{-3}, porosity of 0.46, permeability of 3.82×10^{-15} m^2, residual water saturation of 0.001, and van Genuchten parameter of 0.62. Biogeochemical parameters were taken from literatures or

derived from calibration (Table 5). The remaining biogeochemical parameters can be found in Maggi et al. [2008].

3 Results

3.1 Model testing

TOUGHREACT-N simulated soil moisture content accurately in the 0-17 cm depth during the observation period (Figure 2 a). The soil moisture dynamics have a strong influence on predicted soil aerobicity, as indicated by the lower oxygen concentration in the pore water in the 0-5 and 5-10 cm depth intervals following both irrigation events (Figure 2b). After the first irrigation, microbes quickly consumed the available O_2, turning the soil into anaerobic. As the soil drained, O_2 diffused downward from the atmosphere, and the soil re-oxygenated. Figure 2b indicates that the top 5 cm of soil was more oxic than the deeper (5-10 cm) soil. Relatively low oxygen availability lasted as long as five days in response to each irrigation event. Although soil O_2 concentrations were not measured during the experiment, our predictions are consistent with Sierra and Renault (1998), who observed that the O_2 concentration at 0.2 m depth of a hydromorphic soil decreased 0.09 within 3 days after a rainfall of ≈ 40 mm.

Table 6 provides the model performance statistics for pH and N_2O prediction. For soil pH predictions, the model efficiencies (NSE, Nash and Sutcliffe, 1970) were 0.63, 0.73 and 0.73 for the calibration, validation, and total, respectively. For N_2O emission predictions, the NSE for the calibration, validation, and total were 0.80, 0.46 and 0.62, respectively.

TOUGHREACT-N generally captured the temporal pH patterns resulting from application of different fertilizer forms (Figure 3, R^2=0.73; Figure 5A). Both $(NH_4)_2SO_4$ and NH_4NO_3 fertilizer applications caused a rapid drop of pH due to nitrification followed by a gradual recovery to neutral conditions, while KNO_3 application did not show significant pH decline throughout the simulation period. During the first day after a urea application, there was a rapid rise in soil pH as urea hydrolysis proceeded, followed later by a pH decrease caused by nitrification.

TOUGHREACT-N estimated N_2O fluxes from different fertilizer forms reasonably well, including the onsets, peaks, and decreases over time (Figure 4). Generally, the simulated N_2O flux matched the observations well (R^2 = 0.63; Figure 5B). The second N_2O peaks were relatively poorly estimated compared to the first peaks. We note, however, that the measurement frequency was relatively low, and these peaks in N_2O fluxes may have been missed during sampling. TOUGHREACT-N captured observed cumulative N_2O fluxes very well (Figure 7 a).

Peaks in N_2O flux coincided with fertilizer and irrigation application. N_2O emissions occurred rapidly over the first several days for NH_4NO_3 and $(NH_4)_2SO_4$ applications (Figure 4 a & b). These dynamics were caused by rapid microbial growth (Figure 6) and the accompanying biological reactions stimulated by water and substrate availability. In contrast, N_2O fluxes remained low in KNO_3 due to initially low soil denitrifier abundance. The predicted low N_2O fluxes were consistent with incubation experiments at the Lonchamp site, which showed poor denitrification potential (Henault et al, 1998). In the urea treatment, N_2O fluxes were initially low and then increased strongly starting from the second application. Lower predicted initial N_2O emissions in

the urea treatment were due to the lower availability of NH_4^+-N from urea hydrolysis. This reduced NH_4^+ availability was due to the delay of AOB growth (Figure 6).

The type of fertilizer had a large effect on predicted soil microbial dynamics. In the top 5 cm of soil in the NH_4NO_3, $(NH_4)_2SO_4$, and $CO(NH_2)_2$ treatments, AOB concentration increased initially in response to NH_4^+ supply. In the NH_4NO_3 and $(NH_4)_2SO_4$ treatments, the peak of AOB growth migrated downward because of NO_2^- leaching. In the $CO(NH_2)_2$ treatment the peak AOB concentrations remained near the surface since its solid form did not migrate downward (Figure 6). The absence of NH_4^+ from the KNO_3 fertilizer caused a decline of AOB in the surface soil. DEN biomass in all treatments showed continuous growth on NO_3^- coming either from the input directly (i.e., NH_4NO_3 and KNO_3) or from nitrification (i.e., $CO(NH_2)_2$ and $(NH_4)_2SO_4$) (Figure 6). DENs showed a much smaller peak than AOBs, indicating that the conditions were less favorable for denitrification. As for the AOB, the DEN biomass front migrated downwards in response to NO_3^- leaching. KNO_3 fertilizer application resulted in a maximum growth of DEN's fueled by the large NO_3^-supply.

The 31-day cumulative N-losses were significantly affected by the form of applied N fertilizer (Figure 7). The corresponding N_2O emissions were 690, 879, 527, and 292 g N ha^{-1} for NH_4NO_3, $(NH_4)_2SO_4$, Urea, and KNO_3 fertilizer, respectively, representing 0.28%, 0.36%, 0.21%, and 0.12% of the applied N, respectively. The relation between our predicted cumulative NH_3 emissions are $CO(NH_2)_2$>$(NH_4)_2SO_4$>NH_4NO_3 >KNO_3 (Figure 7 b). The leachate fluxes were computed at 20 cm depth due to the short simulation period of this study. The order of cumulative N-leaching from fertilizer types depended on NO_3^- concentration depth.

Consequently, KNO_3 fertilization led to the maximum leaching fluxes followed by NH_4NO_3, $(NH_4)_2SO_4$, and $CO(NH_2)_2$ fertilizers (Figure 7 e). $CO(NH_2)_2$ had the least NO_2^- and NO_3^- leaching among all the fertilizer forms because of its slow production of NO_2^- and NO_3^- from nitrification.

Our results showed that cumulative NO and N_2O emissions following nitrate fertilizer (i.e., KNO_3) application were two to three times lower than from ammonium-N fertilizers. The differences were due to differences in nitrification rates with higher activity in soils receiving an NH_4^+ fertilizer, which is confirmed by higher AOB biomass than DEN biomass (Figure 6). To better understand the interactions and mechanisms leading to N_2O emissions, we performed a series of sensitivity analyses to characterize how fertilizer type and amount, irrigation, and soil type impact cumulative N emissions in this system.

3.2 Fertilizer Amount

The N biogeochemical cycle depends primarily on substrate availability and interaction among microbial populations. The increase of NH_4^+ and NO_3^- from fertilizer induces higher rates of microbially-induced nitrification and denitrification. These increases in reaction rates, however, can be different depending on the affinities of microbes to substrates. Thus, the disproportionate biogeochemical reaction rates may cause different changes in relative N-losses between fertilizer-type treatments. To illustrate these relationships, we calculated the cumulative N losses for fertilizer application rates increasing from 50 to 400 kg N ha^{-1} (100 kg N ha^{-1} corresponds to the reference application).

Cumulative N-losses depended strongly on fertilizer amount (Figure 8a), primarily by impacting substrate supply. NH_3 volatilization from $CO(NH_2)_2$ increased more than those from NH_4NO_3 and $(NH_4)_2SO_4$ fertilizers because the alkalinity effect by $CO(NH_2)_2$ accelerates NH_3 volatilization. Negligible NH_3 emissions were predicted for KNO_3 fertilizer due to the absence of NH_4^+. Consequently, the differences in cumulative NH_3 volatilization between $CO(NH_2)_2$ and other fertilizers increased with fertilizer amount. $CO(NH_2)_2$ fertilization emitted 8.8 and 40 times more NH_3 than NH_4NO_3 fertilizer under the 50 and 400 kg N ha^{-1} treatments, respectively.

Increasing fertilizer amount diminished differences in cumulative NO and N_2O emissions from different fertilizer types (Figure 8b). In other words, cumulative NO and N_2O emissions under $CO(NH_2)_2$ fertilization increased with fertilizer amounts more rapidly than under NH_4NO_3 and $(NH_4)_2SO_4$ fertilization because the alkalinity induced by $CO(NH_2)_2$ relieves microbial acidity stress. Under the 50 kg N ha^{-1} treatment, NH_4^+ fertilizer emitted 1.6 times more NO than $CO(NH_2)_2$ fertilizer, while only 1.2 times higher than $CO(NH_2)_2$ under the 400 kg N ha^{-1} treatment. Similarly, $CO(NH_2)_2$ showed a more rapid increase of cumulative N_2O emissions with increased fertilizer amount than other fertilizer treatments. Consequently, at higher fertilizer application rates (i.e., >200 kg N/ha), urea had the highest N_2O emissions among all fertilizers tested here.

In contrast, increasing fertilizer amount exaggerated the difference of cumulative solute leaching from fertilizer types (Figure 8). For example, NO_3^- leaching from KNO_3 is 13 and 1.7 times higher than $(NH_4)_2SO_4$ and NH_4NO_3, respectively, in the 400 kg N ha^{-1} treatment, compared to 7 and 1.2 times in the 100 kg N ha^{-1} treatment (**Figure 8** e).

3.3 Effect of soil pH

Soil pH significantly impacted microbial dynamics and therefore the N cycle. Additionally, pH is subject to a feedback by which protons are consumed and produced during biogeochemical processes. One of the advantages of TOUGHREACT-N is its mechanistic representation of pH dynamics. For simplicity, we considered only calcite content among many potential buffers (e.g., ion exchange capacity, etc.) to study soil pH effect on N cycling. Soil pH and $CaCO_3$ content are coupled due to the buffering capacity of $CaCO_3$, i.e., increases in $CaCO_3$ content lead to increases in soil buffering capacity. The predicted faster microbial growth rates in high calcite fraction soils correlated to a reduction of acidity stress on microbes (not shown). Predicted relative impacts of fertilizer type on NH_3 emissions did not change significantly with soil buffering capacity (Figure 9 a). The NO emission from the NH_4^+-fertilizers decreased with increasing calcite content, which we attributed to NO produced by chemodenitrification [*Venterea and Rolston*, 2000b] at low pH. The change, however, is small relative to the change in N_2O emissions (Figure 9 b and c) because of the contrasting effects of increasing pH on chemodenitrification and the microbial production of NO.

The dynamics of soil pH was influenced by soil buffering capacity (i.e., calcite fraction) and had significant impacts on cumulative N_2O losses, with predicted three- and five-fold increases for NH_4NO_3 and $(NH_4)_2SO_4$ as calcite fraction increased from 0.02% to 0.5% (Figure 9 c). Compared to the reference case, the model simulated a larger variation of N_2O fluxes at 0.5% calcite fraction (1975, 3756, 411, and 508 kg N ha^{-1} for NH_4NO_3, $(NH_4)_2SO_4$, urea, and KNO_3, respectively). Thus, in soils with high calcite content, and therefore more buffered against pH changes, NH_4^+ fertilizer would be

expected to emit much more N_2O gas than $CO(NH_2)_2$ and NO_3^- fertilizers for the same fertilizer amount.

Differences in cumulative N leaching between fertilizer types decreased with increasing soil calcite fraction (Figure 9). The decreasing N-leaching with increasing calcite fraction was due to enhanced denitrification that depleted the NO_3^- pool in the upper soil layers. The enhanced denitrification rate at 0.5% calcite content induced attenuated NO_3^- fronts in vertical profiles compared to those at 0.02% calcite content (not shown).

TOUGHREACT-N predicted different N_2O gas emissions and N_2O/N_2 ratios as a function of initial soil pH for NO_3^- and NH_4^+ fertilizer treatments and two soil types: a clay loam (Figure A) and a sandy loam (Figure B). These simulations were run by removing the soil buffering capacities (i.e., calcite content and ion exchange capacity), which would otherwise mask effects of initial pH. Generally, the N_2O emissions and the response to pH changes for clay loam were larger than those for the sandy loam. N_2O emissions increased nonlinearly with soil pH with a 6-fold increase for a pH change from 5 to 7 in sandy loam (Figure). The N_2O/N_2 emission ratio negatively correlated with pH for clay loam, and showed a maximum at pH of 6 for sandy loam soil. The N_2O emission and N_2O /N_2 of the NH_4^+ treatment were more sensitive to pH change than the NO_3^- treatment.

4 Discussion

Simulated NH_3-N loss from the Longchamp site is significantly affected by fertilizer types. NH_3 volatilization depended on: (1) the NH_4^+ concentration developed at

the soil surface and (2) the changes in pH that were controlled by the fertilizer application, soil buffering capacity, and microbial activity [*Mkhabela et al.*, 2006]. The first factor, NH_4^+ concentration, was the dominant reason for which ammonium-N fertilizers had much higher potential for ammonia to volatilize compared to nitrate-N fertilizer. The second factor, pH, directly affected the equilibrium between NH_4^+ and NH_3. Thus, the alkaline reactions of urea hydrolysis resulted in an increase in pH and a significant NH_3 volatilization (one order of magnitude higher than other fertilizer types) (Figure 7 b). The simulated low NH_3 volatilization in the current study was due to the acidic soil and high soil cation exchange capacity (CEC). Where the soil was buffered at pH values less than ~7, the dominant form of ammonia-N was NH_4^+ and the potential for volatilization was small. Large soil CEC (i.e., high NH_4^+ adsorption) tended to reduce NH_3 volatilization potential by reducing the NH_4^+ soil solution concentration on exchange sites and by reducing pH (i.e., releasing H^+).

The effects of fertilizer forms on N gas emissions and NO_3^- leaching were strongly dependent on soil properties. Soil texture impacts soil moisture, which directly influenced gas diffusion and soil oxygen availability. As a result, nitrification was the predominant source of NO and N_2O emissions in coarse texture soils. Consequently, the availability of substrate for nitrification (i.e., NH_4^+) determined the magnitude of nitrogen gas emissions. N_2O emission from nitrate fertilizer (i.e., KNO_3) was shown to be lower than from ammonium fertilizers in sandy soils (Figure 10 B.). Our simulations also showed higher N_2O emissions associated with clay loam than sandy soil regardless of the form of N input. This prediction was consistent with experimental observations which have shown that fine textured soils and restricted drainage favor N_2O emissions [*Velthof*

and Oenema, 1995]. The lower hydraulic conductivity of the fine textured soil (i.e., clay loam) led to slower drainage rates and higher soil moisture than in the sandy loam soils. The higher soil moisture increased the period where soil O_2 was depleted, leading to enhancements in denitrification rates and NO and N_2O emissions. Thus, nitrate-N fertilizer may reduce NO and N_2O emissions (but not N-leaching) in well-aerated soils, while ammonium-N fertilizers may be more suitable to poorly-drained soils.

Soil pH had a large influence on predicted N losses by impacting the three most important processes that generate nitrogen gases: nitrifier denitrification, chemodenitrification, and denitrification. On the one hand, simulations showed that cumulative NO emissions under field capacity conditions decreased with increasing calcite content. Lower initial acidity decreased abiotic NO production, which are typically more important under acidic conditions (e.g., HNO_2 decompostion). On the other hand, our study showed that the cumulative N_2O emission increased with increasing calcite content (Figure 9). This latter result is in agreement with Clough et al. [2004], who found increasing N_2O emissions in response to increasing pH at saturated soils from a urine patch. Increasing denitrification along increasing pH due to acidity stress release would exceed any effect of decreasing abiotic N-gas production.

The current N- biogeochemical models are based upon the assumption of products ratios (i.e.N_2O/N_2) independent of soil pH (Parton et al., 1996, Li, et al., 2000). In contrast, our study demonstrates that N trace-gas speciation depends on pH, N-substrate, and soil properties. This behavior emerges because N gas effluxes depend on the substrate and the soil pH before and after fertilization. Soil pH dynamics is determined by the biogeochemical reactions (which are also a function of pH), and soil buffering

capacity. Also, soil oxygen and substrate availability depend on biogeochemical reactions and soil hydrological properties that influence soil moisture and advection and diffusive transport. As a result, N gas effluxes are related non-linearly to soil pH, soil properties, and N-substrate form and concentration. Our simulation results showed that these ratios depend on soil pH, N-substrate, and soil texture. Thus the validity of applying empirically derived predictive functions based on constant fraction of N species is questionable. The approach presented here allows us to mechanistically quantify the interaction of multiple N-cycle controlling processes under large temporal and spatial variability.

5 Conclusions

We further developed and tested the N biogeochemical model TOUGHREACT-N by including application of different mineral N fertilizers, and water and chemical transport mechanisms (e.g. water percolation, chemical phase partitioning, advection, and diffusion, etc). We then applied TOUGHREACT-N to an agricultural field experiment in Burgundy, France. The model performed well and showed great promise in modeling NO, N_2O, and NH_3 emissions and NO_3^- leaching from agro-ecosystems undergoing fertilization and irrigation.

Model simulations showed the relation between N losses, fertilizer type, fertilization practices, and soil conditions. The results that have direct implications to fertilizer management practices include. (i) soils receiving relatively small amounts of fertilizer (<100 kg N ha^{-1}) produced more N emissions per applied N but slightly less N leaching from NH_4^+ than NO_3^- fertilizers; this difference was diminished at higher fertilization rates. Urea may produce maximum N emissions at higher fertilization rates.

Consequently, the effect of a given reduction in N input on nitrogen gases emissions will be larger for urea than for other NH_4^+ and NO_3^- based fertilizers. (ii) soil buffering capacity dramatically increased N_2O emissions after fertilization; increasing alkalinity can increase NH_3 volatilization and (iii) soils with coarse texture produced less nitrogen gas emissions from NO_3^- fertilizers than NH_4^+ fertilizers. Practically, any gains that may be made in reducing one N-species loss also need to be considered in the context of possible changes to other N-species. Mitigation approaches that do not include these tradeoffs may lead to unanticipated environmental problems.

Our work highlights the need for improvement of the N_2O emissions inventory methodology, which currently relies on a constant emission factor irrespective of fertilizer types, environmental conditions, and soil properties. The results presented here suggest that even fertilizer-type specific emission factors need to be a function of soil type and management practice (e.g. fertilization amount).

The development of simplified mechanistic models for regional scale application remains our goal of this research. Further coupling with atmospheric forcing (e.g., solar radiation, wind speed) and plant growth is the essential model component that needs to be accomplished. However, the current TOUGHREACT may serve as the theoretical basis for more complex large scale models which incorporate plant growth, C and N cycling, climate, and agricultural management practices.

Acknowledgments.

This work was supported by Laboratory Directed Research and Development (LDRD)

funding from Berkeley Lab, provided by the Director, Office of Science, of the U.S. Department of Energy under Contract No. DE-AC02-05CH11231. Dr. Catherine Henault is thanked for providing data and information at Longchamp site. The authors also acknowledge Yoram Rubin (University of California, Berkeley) and Bo Bodvarsson (Lawrence Berkeley National Laboratory) for making this project possible.

5 References

Aber, J., McDowell, W., Nadelhoffer, K., Magill, A., Berntson, G., Kamakea, M., McNulty, S., Currie, W., Rustad, L., & Fernandez, I. (1998). Nitrogen saturation in temperate forest ecosystems - Hypotheses revisited. *Bioscience 48*, 921-934.

Ahuja, L.R., Rojas, K.W., Hanson, J.D., Shaffer, M.J., Ma, L., 2000. Root Zone Water Quality Model: Modelling Management Effects on Water Quality and Crop Production. Water Resources Publicatins, LLC, Highlands Ranch, CO, 372 pp.

Appelo, C.A.J., & Postma, D. (1993). *Geochemistry, groundwater and pollution*. Rotterdam, The Netherlands: Balkema, 536 pp.

Blackmer, A.M., Robbins, S.G., & Bremner, J.M. (1982). Diurnal Variability in Rate of Emission of Nitrous-Oxide from Soils. *Soil Science Society of America Journal 46*, 937-942.

Bremner, J.M. (1997). Sources of nitrous oxide in soils. *Nutrient Cycling in Agroecosystems 49*, 7-16.

Byrnes, B.H. (1990). Environmental-Effects of N Fertilizer Use - an Overview. *Fertilizer Research 26*, 209-215.

Clayton, H., McTaggart, I.P., Parker, J., Swan, L., & Smith, K.A. (1997). Nitrous oxide emissions from fertilised grassland: A 2-year study of the effects of N fertiliser form and environmental conditions. *Biology and Fertility of Soils 25*, 252-260.

Clough, T.J., Kelliher, F.M., Sherlock, R.R., & Ford, C.D. (2004). Lime and soil moisture effects on nitrous oxide emissions from a urine patch. *Soil Science Society of America Journal 68*, 1600-1609.

Conrad, R. (1996). Soil microorganisms as controllers of atmospheric trace gases (H_2, CO, CH_4, OCS, N_2O, and NO). *Microbiological Reviews 60*, 609-&.

Davidson, E.A., Vitousek, P.M., Matson, P.A., Riley, R., Garciamendez, G., & Maass, J.M. (1991). Soil Emissions of Nitric-Oxide in a Seasonally Dry Tropical Forest of Mexico. *Journal of Geophysical Research-Atmospheres 96*, 15439-15445.

Eichner, M.J. (1990). Nitrous oxide emissions from fertilized soils: Summary of available data. *Journal of Environmental Quality ; Vol/Issue: 19:2*, Pages: 272-280.

Flessa, H., Dorsch, P., & Beese, F. (1995). Seasonal-Variation of N_2O and CH_4 Fluxes in Differently Managed Arable Soils in Southern Germany. *Journal of Geophysical Research-Atmospheres 100*, 23115-23124.

Firestone MK, Davidson EA (1989) In: Andrease MO, Schimel DS (des) Microbiological basis of NO and N2O production and consumption in soil. pp7-21.

Frolking, S.E., Mosier, A.R., Ojima, D.S., Li, C., Parton, W.J., Potter, C.S., Priesack, E., Stenger, R., Haberbosch, C., Dorsch, P., Flessa, H., & Smith, K.A. (1998). Comparison of N_2O emissions from soils at three temperate agricultural sites: simulations of year-round measurements by four models. *Nutrient Cycling in Agroecosystems 52*, 77-105.

Galloway, J.N., Aber, J.D., Erisman, J.W., Seitzinger, S.P., Howarth, R.W., Cowling, E.B., & Cosby, B.J. (2003). The nitrogen cascade. *Bioscience 53*, 341-356.

Gbondo-Tugbawa, S.S., C.T. Driscoll , J.D. Aber and G.E. Likens. (2001).The evaluation of an integrated biogeochemical model (PnET-BGC) at a northern hardwood forest ecosystem. Water Resources Research 37:1057-1070

Grant, R.F., Nyborg, M., & Laidlaw, J.W. (1993). Evolution of Nitrous-Oxide from Soil .1. Model Development. *Soil Science 156*, 259-265.

Hall, S.J., Matson, P.A., & Roth, P.M. (1996). NO_x emissions from soil: Implications for air quality modeling in agricultural regions. *Annual Review of Energy and the Environment 21*, 311-346.

Harbaugh, A.W., McDonald, M.G. (1996). User's Documentation for MODFLOW-96, an update to the US Geological Survey modular finite-difference groundwater model, US Geol. Surv. OpenFile Rep. 96-485.

Henault, C., Devis, X., Lucas, J.L., & Germon, J.C. (1998). Influence of different agricultural practices (type of crop, form of N-fertilizer) on soil nitrous oxide emissions. *Biology and Fertility of Soils 27*, 299-306.

Hill, A.R. (1996). Nitrate removal in stream riparian zones. *Journal of Environmental Quality 25*, 743-755.

Hutchinson, G.L., Guenzi, W.D., & Livingston, G.P. (1993). Soil-Water Controls on Aerobic Soil Emission of Gaseous Nitrogen-Oxides. *Soil Biology & Biochemistry 25*, 1-9.

Hutchinson, G.L., Vigil, M.F., Doran, J.W., & Kessavalou, A. (1997). Coarse-scale soil-atmosphere NO_X exchange modeling: Status and limitations. *Nutrient Cycling in Agroecosystems 48*, 25-35.

IPCC. (2001). *Intergovernmental Panel on Climate Change* Cambridge: Cambridge University Press.

Jardine, P.M., Dunnivant, F.M., Selim, H.M., & McCarthy, J.F. (1992). Comparison of Models for Describing the Transport of Dissolved Organic-Carbon in Aquifer Columns. *Soil Science Society of America Journal 56*, 393-401.

Jiao, Y., Hendershot, W.H., & Whalen, J.K. (2004). Agricultural practices influence dissolved nutrients leaching through intact soil cores. *Soil Science Society of America Journal 68*, 2058-2068.

Kroeze, C., Aerts, R., van Breemen, N., van Dam, D., van der Hoek, K., Hofschreuder, P., Hoosbeek, M., de Klein, J., Kros, H., van Oene, H., Oenema, O., Tietema, A., van der Veeren, R., & de Vries, W. (2003). Uncertainties in the fate of nitrogen I: An

overview of sources of uncertainty illustrated with a Dutch case study. *Nutrient Cycling in Agroecosystems 66*, 43-69.

Leffelaar, P.A., & Wessel, W.W. (1988). Denitrification in a Homogeneous, Closed System - Experiment and Simulation. *Soil Science 146*, 335-349.

Leonard, R.A., Knisel, W.G., Still, D.S., 1987. GLEAMS: groundwater loading effects of agricultural management systems. Trans. ASAE 30, 1403-1418.

Li, C.S., Frolking, S., & Frolking, T.A. (1992). A Model of Nitrous-Oxide Evolution from Soil Driven by Rainfall Events .1. Model Structure and Sensitivity. *Journal of Geophysical Research-Atmospheres 97*, 9759-9776.

Lowrance, R., Altier, L.S., Newbold, J.D., Schnabel, R.R., Groffman, P.M., Denver, J.M., Correll, D.L., Gilliam, J.W., Robinson, J.L., Brinsfield, R.B., Staver, K.W., Lucas, W., & Todd, A.H. (1997). Water quality functions of Riparian forest buffers in Chesapeake Bay watersheds. *Environmental Management 21*, 687-712.

Maggi,F., Gu,C., Riley,W.J., Venterea,R., Hornberger,G.M., Venterea, R.T., Xu, T., Spycher, N., Steefel, C., Miller, N.L., Oldenburg, C.M. (2008) A mechanistic treatment of the dominant soil nitrogen cycling processes: Model development, testing, and application. Journal of Geophysical Research-Biogeosciences 113, G02016, doi:10.1029/2007JG000578.

Mcconnaughey, P.K., & Bouldin, D.R. (1985). Transient Microsite Models of Denitrification .1. Model Development. *Soil Science Society of America Journal 49*, 886-891.

McKenney, D.J., & Drury, C.F. (1997). Nitric oxide production in agricultural soils. *Global Change Biology 3*, 317-326.

McTaggart, I.P., Akiyama, H., Tsuruta, H., & Ball, B.C. (2002). Influence of soil physical properties, fertiliser type and moisture tension on N_2O and NO emissions from nearly saturated Japanese upland soils. *Nutrient Cycling in Agroecosystems 63*, 207-217.

Mkhabela, M.S., Gordon, R., Burton, D., Madani, A., Hart, W., & Elmi, A. (2006). Ammonia and nitrous oxide emissions from two acidic soils of Nova Scotia fertilised with liquid hog manure mixed with or without dicyandiamide. *Chemosphere 65*, 1381-1387.

Parton, W.J., Mosier, A.R., Ojima, D.S., Valentine, D.W., Schimel, D.S., Weier, K., & Kulmala, A.E. (1996). Generalized model for N_2 and N_2O production from nitrification and denitrification. *Global Biogeochemical Cycles 10*, 401-412.

Parton, w.J., Holland, E.A., Del Grosso, S.J., Hartman, M.D., Martin, R.E., Mosier, A.R., Ojima, D.D., Schimel, D.S., 2001. Generalized model for NO_x and N2O emissions from soils. J.Geophys.Res. 106 (D15), 17403-17419.

Pruess, K., Oldenburg, C.M., & Moridis, G. (1999). TOUGH2 Users Guide. Berkeley, CA: Lawrence Berkeley National Laboratory.

Refsgaard, J.C., Storm, B., (1995). MIKE SHE. In: Singh, V.P. (Ed.), Computer Models of Watershed Hydrology. Water Resources Publication, pp.809-846.

Riley, W.J., & Matson, P.A. (2000). NLOSS: A mechanistic model of denitrified N_2O and N_2 evolution from soil. *Soil Science 165*, 237-249.

Running, S.W. and S.T. Gower (1991) FOREST-BGC, a general model of forest ecosystem processes for regional applications, II. Dynamic carbon allocation and nitrogen budgets. Tree Physiol., 9, 147-160.

Scanlon, B.R., Jolly, I., Sophocleous, M., & Zhang, L. (2007). Global impacts of conversions from natural to agricultural ecosystems on water resources: Quantity versus quality. *Water Resources Research 43*, -.

Scanlon, T.M., & Kiely, G. (2003). Ecosystem-scale measurements of nitrous oxide fluxes for an intensely grazed, fertilized grassland. *Geophysical Research Letters 30*.

Skiba, U., Fowler, D., & Smith, K.A. (1997). Nitric oxide emissions from agricultural soils in temperate and tropical climates: sources, controls and mitigation options. *Nutrient Cycling in Agroecosystems 48*, 139-153.

Thornton, P. E., S. W. Running, and E. R. Hunt. (2005). Biome-BGC: Terrestrial Ecosystem Process Model, Version 4.1.1. Model product. Available on-line [http://www.daac.ornl.gov] from Oak Ridge National Laboratory Distributed Active Archive Center, Oak Ridge, Tennessee, U.S.A. doi:10.3334/ORNLDAAC/805.

vanderWeerden, T.J., & Jarvis, S.C. (1997). Ammonia emission factors for N fertilizers applied to two contrasting grassland soils. *Environmental Pollution 95*, 205-211.

Velthof, G.L., & Oenema, O. (1995). Nitrous oxide fluxes from grassland in the Netherlands .2. Effects of soil type, nitrogen fertilizer application and grazing. *European Journal of Soil Science 46*, 541-549.

Venterea, R.T., & Rolston, D.E. (2000a). Mechanistic modeling of nitrite accumulation and nitrogen oxide gas emissions during nitrification. *Journal of Environmental Quality 29*, 1741-1751.

Venterea, R.T., & Rolston, D.E. (2000b). Nitric and nitrous oxide emissions following fertilizer application to agricultural soil: Biotic and abiotic mechanisms and kinetics. *Journal of Geophysical Research-Atmospheres 105*, 15117-15129.

Vitousek, P.M., Aber,J.D., Howarth, R.W., Likens, G.E. (1997). Human alteration of the global nitrogen cycle: Sources and consequences. Ecol. Appl. 7:737-750.

Xu, T., Sonnenthal, E., Spycher, N., & Pruess, K. (2005). TOUGHREACT users guide: a simulation program for non-isothermal multiphase reactive geochemical transport in variable saturated geologic media. Berkeley,CA: Lawrence Berkeley National Laboratory.

Yienger, J.J., & Levy, H. (1995). Empirical-Model of Global Soil-Biogenic NO_x Emissions. *Journal of Geophysical Research-Atmospheres 100*, 11447-11464.

Youssef, M.A., Skaggs, R.W., Chescheir, G.M., & Gilliam, J.W. (2005). The nitrogen simulation model, DRAINMOD-N II. *Transactions of the Asae 48*, 611-626.

Zheng, C., Wang, P.P., 1999. MT3DMS: a modular three-dimensional multispecies transport model for simulation of advection, dispersion, and chemical reactions of contaminants in groundwater systems; documentation and user's guide SERDP-99-1. US Army Corps of Engineers, Washington, DC.

Table 1. Summary of N-biogeochemical processes simulated in TOUGHREACT-N

Reaction	Nitrification	Denitrification	Nitrifier denitrification	Chemo denitrification	Aerobic respiration
Micro organism	AOB[1] &NOB[2]	DEN[3]	AOB[1]	None	AER[4]& DEN[3]
Substrate	NH_4^+,NO_2^-, O_2	DOC, NO_3^-, NO_2^-, NO and N_2O	DOC, NO_2^-, NO and N_2O	HNO_2	DOC, O_2

[1]-Amonium Oxidizer Bacteria; [2]-Nitrite oxidizer Bacteria; [3]-Denitrifier; [4]-Aerobes

Table 2. Chemical Species Considered in the Model

Group	Species
Primary species	H_2O, CH_2O, H^+, $O_2(aq)$, NH_4^+, NO_3^-, NO_2^-, $NO(aq)$, N_2O (aq), $N_2(aq)$, HCO_3^-, Ca^{2+}, K^+, SO_4^{2-}, $CO(NH_2)_2$
Aqueous complexes	OH^-, HNO_2, HNO_3, $NH_3(aq)$, CO_3^{2-}, $CO_2(aq)$, $CaCO_3^0$, $CaHCO_3^+$, $CaSO_4^0$, HSO_4^-, KSO_4^-
Precipitated species	$CaCO_3$, $CaSO_4$
Gaseous species	$O_2(g)$, $NO(g)$, $N_2O(g)$, $N_2(g)$, $CO_2(g)$, $NH_3(g)$

Table 3. Initial chemical N concentrations for four fertilizer types at 0-1.25 cm depth.

Fertilizer Types		*NH_4NO_3*	*$(NH_4)_2SO_4$*	*$CO(NH_2)_2$*	*KNO_3*
NH_4^+	10^{-1}[mol L^{-1}]	0.77	1.54	1×10^{-5}	1×10^{-2}
NO_3^-	10^{-1}[mol L^{-1}]	0.77	1×10^{-2}	1×10^{-2}	1.54
K^+	10^{-1}[mol L^{-1}]	1×10^{-2}	1×10^{-2}	1×10^{-2}	1.54
$CO(NH_2)_2$	10^{-1} [mol L^{-}	1×10^{-5}	1×10^{-5}	0.77	1×10^{-5}
SO_4^{-2}	10^{-1}[mol L^{-1}]	1×10^{-2}	0.77	1×10^{-2}	1×10^{-2}

Table 4. Initial conditions of water saturation and aqueous concentrations of all primary species other than fertilizer chemicals (note: water saturation IC's the same for all fertilizer treatments). Values of the species marked with † were assigned by steady-state simulation without N-species. Values of the species marked with * were calibrated with observations.

Depth Interval		*0-1.25 (cm)*	*1.25-10 (cm)*	*10-60 (cm)*
S_θ*		0.82	0.82	0.80
pH		6.0	6.0	7.0
O_2 (aq)	10^{-4}[mol L^{-1}]	2.7	2.7	2.7
NO_2^-	10^{-6}[mol L^{-1}]	1.0	1.0	1.0
NO (aq)	10^{-6}[mol L^{-1}]	1.0	1.0	1.0
N_2O (aq)	10^{-6}[mol L^{-1}]	1.0	1.0	1.0
N_2 (aq)	10^{-6}[mol L^{-1}]	1.0	1.0	1.0
HCO_3^-†	10^{-2}[mol L^{-1}]	4.76	4.76	4.76
Ca^{2+}†	10^{-2}[mol L^{-1}]	2.76	2.11	2.11
POC	10^{3}[mol L^{-1}]	1.5	1.5	0.78
AOB*	10^{1}[mol L^{-1}]	1.26	1.07	0.52
NOB*	[mol L^{-1}]	3.5	3.2	0.5
DEN*	[mol L^{-1}]	5.0	3.1	1.6
AER*	10^{1}[mol L^{-1}]	7.3	6.2	1.0

Table 5. Biogeochemical parameters. Parameters marked with * were calibrated values

Parameters [unit]	Definition	value
$\delta_{AER}{}^{*}[s^{-1}]$	Aerobes death rate	2.16×10^{-6}
$\mu_{AER}{}^{*}[s^{-1}]$	Maximum Aerobic Respiration rate	7.69×10^{-6}
$\mu_{AOB}{}^{*}[s^{-1}]$	Maximum growth rate of AOB	1.29×10^{-5}
$\mu_{NOB}{}^{*}[s^{-1}]$	Maximum growth rate of NOB	8.78×10^{-6}
$\mu_{DEN-NO_3^-}{}^{*}[s^{-1}]$	Maximum growth rate of NO_3^- DEN	1.75×10^{-5}
$\mu_{DEN-NO_2^-}{}^{*}[s^{-1}]$	Maximum growth rate of NO_2^- DEN	1.70×10^{-5}
$\mu_{DEN-NO}{}^{*}[s^{-1}]$	Maximum growth rate of NO DEN	8.30×10^{-6}
$\mu_{DEN-N_2O}{}^{*}[s^{-1}]$	Maximum growth rate of N_2O DEN	8.37×10^{-6}
μ_u $[\mu gN\ g^{-1}soil\ d^{-1}]$	Maximum urea dissolution rate	120 [Youssef et al., 2005]
K_u $[mg\ L^{-1}]$	Half saturation constant for urea hydrolysis	50 [Youssef et al., 2005]
$CaCO_3$ fraction		0.02%
α^{*} $[s^{-1}]$	1st order mass transfer coefficient of POC	4.21×10^{-7}[Jardine et al., 1992]
K_d $[Lkg^{-1}]$	Distribution coefficient of DOC	50 [Jardine et al., 1992]
CEC *[meq/100g solid]*	Cation exchange capacity	3.23

Table 6 Model performance of simulated pH and N_2O emission for the calibration , validation, and total, respectively

Nash-Sutcliffe efficiency coefficient	Calibration	Validation	Total
pH	0.63	0.73	0.73
N_2O	0.80	0.46	0.62

Figure legends

Figure 1 Schematic representation of the chain of biochemical nitrification and denitrification reactions (left side) and microbial respirations (right side). Mineral, liquid, and gaseous domains are separated by dashed lines. AOB, NOB, DEN, and AER stand for ammonia oxidizing bacteria, nitrite oxidizing bacteria, denitrifying bacteria, and aerobic bacteria, respectively [Maggi, et.al, 2008]

Figure 2. (a) Observed and simulated water-filled pore space (WFPS) and (b) simulated dissolved oxygen concentration between 0-5 and 5-10 cm depth intervals over the simulation period. Two irrigation events are indicated by downward arrows.

Figure 3. Time evolution of observed and simulated soil pH of 0-20 cm layer over the simulation period (line-simulation, symbol-experiment).

Figure 4. Observed and modeled time evolution of N_2O (g) emissions. Two application/irrigation events occurred at day 0 and day 15, respectively, indicated by downward arrows.

Figure 5 The observed vs. simulated A) pH and B) N_2O flux

Figure 6. Predicted vertical distribution of Ammonium Oxidizer Bacteria (AOB) and Denitrifier (DEN) over time. AOB and DEN dynamics reflected the interaction with N transport in space and transformation in time.

Figure 7. Time cumulative (a) N_2O, (b) NH_3, (c) NO, and (d) N_2 gases emissions and (e) NO_2^-+NO_3^- leachate fluxes at 20 cm depth as a function of fertilizer types.

Figure 8. Time cumulative (a) NH_3, (b) NO, and (c) N_2O surface fluxes to the atmosphere, and (d) NO_2^- and (e) NO_3^- leachate fluxes at 20 cm for the four fertilizer types as functions of fertilizer amount. The NH_3 volatilization from KNO_3 and the leachate fluxes from $CO(NH_2)_2$ were negligible and thus omitted. The reference case is 100 kg N ha^{-1}. The figure is shown with a semi-log scale to illustrate the differences changes by detecting divergence or convergence of curves.

Figure 9. Time cumulative (a) NH_3, (b) NO, and (c) N_2O surface fluxes to the atmosphere, and (d) NO_2^- and (e) NO_3^- leachate fluxes at depth of 20 cm for the four fertilizer types as functions of soil calcite fraction. The NH_3 volatilization from KNO_3 and the leachate fluxes from $CO(NH_2)_2$ were negligible and thus omitted.

Figure 10 Predicted N_2O flux and N_2O/N_2 ratio from NO_3^- or NH_4^+ treatments as a function of soil pH. Solid lines indicate N_2O flux and dash lines indicate N_2O/N_2 ratio. Thick lines indicate NH_4^+ treatment and thin lines indicate NO_3^- treatment. The figures shown correspond to two soils: A) clay loam and B) sandy loam

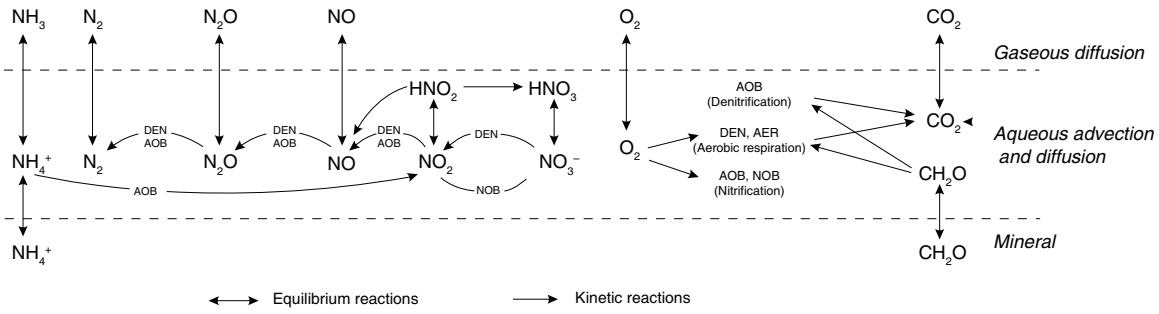

Figure 1 Schematic representation of the chain of biochemical nitrification and denitrification reactions (left side) and microbial respirations (right side). Mineral, liquid, and gaseous domains are separated by dashed lines. AOB, NOB, DEN, and AER stand for ammonia oxidizing bacteria, nitrite oxidizing bacteria, denitrifying bacteria, and aerobic bacteria, respectively [Maggi, et.al, 2008]

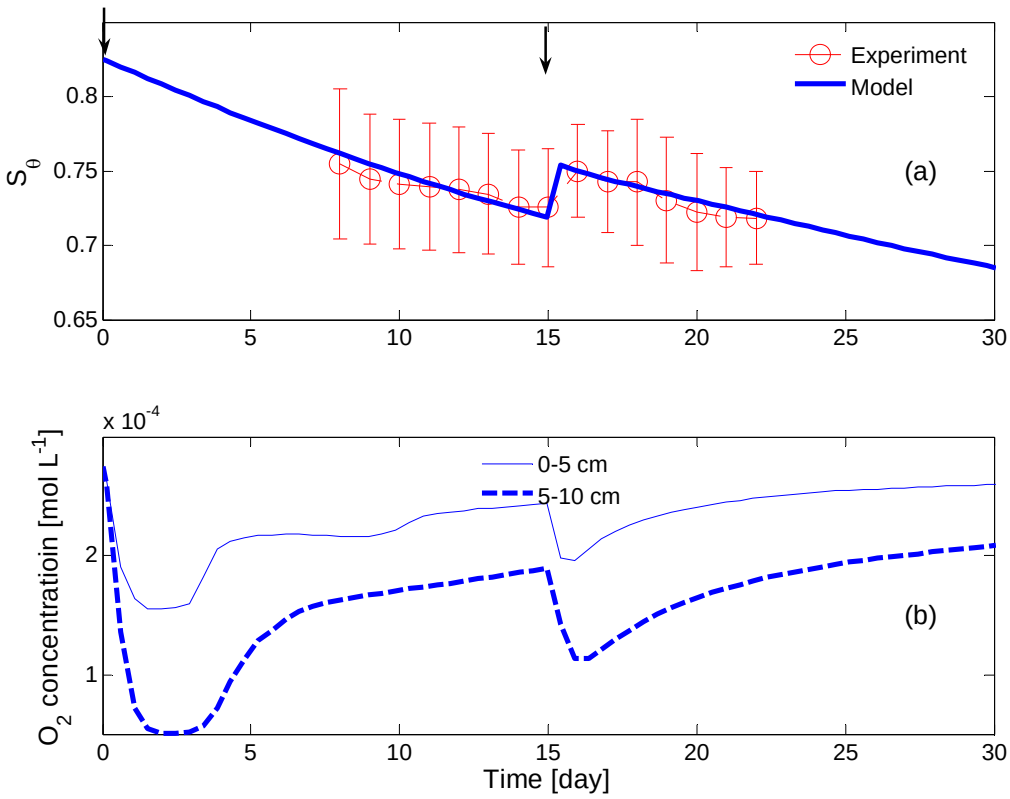

Figure 2 (a) Observed and simulated water-filled pore space (WFPS) and (b) simulated dissolved oxygen concentration between 0-5 and 5-10 cm depth intervals over the simulation period. Two irrigation events are indicated by downward arrows.

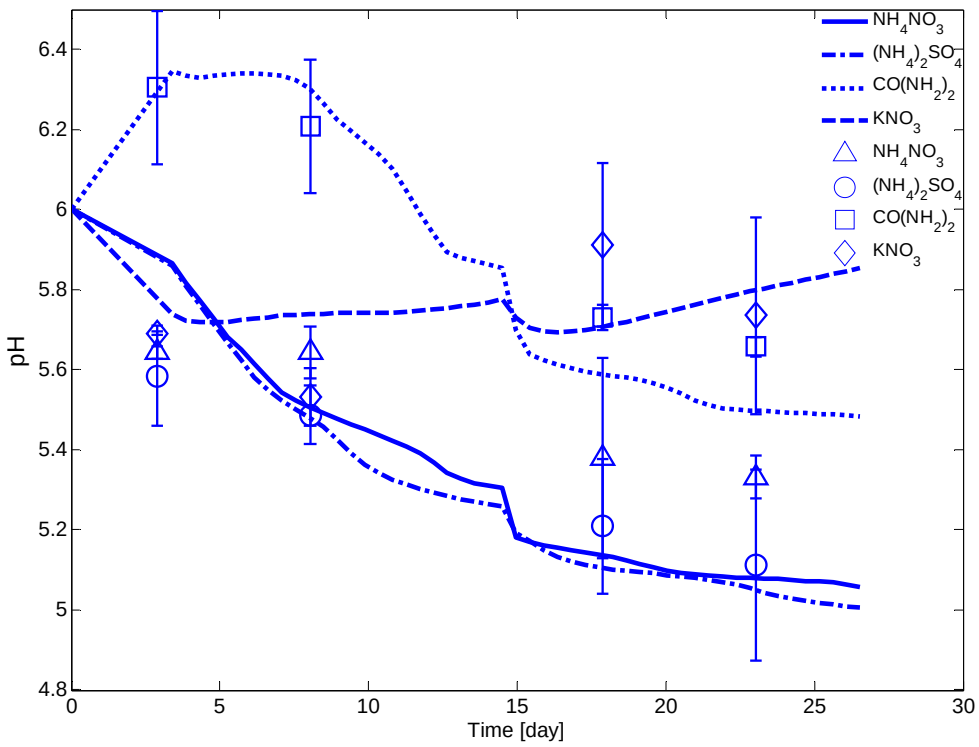

Figure 3 Time evolution of observed and simulated soil pH of 0-20 cm layer over the simulation period (line-simulation, symbol-experiment).

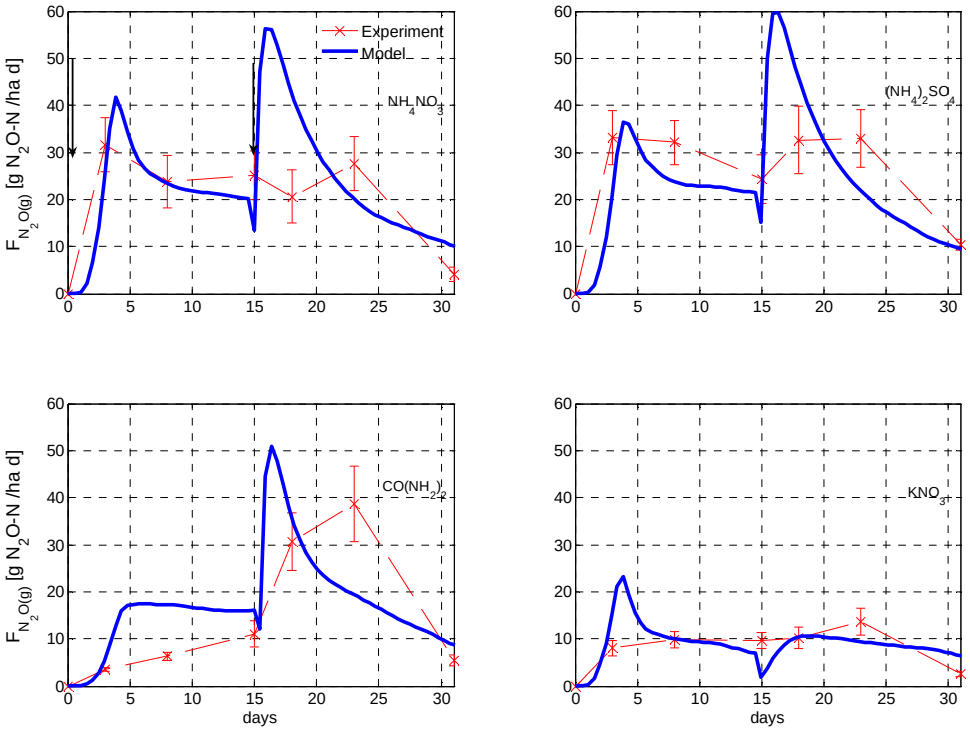

Figure 4. Observed and modeled time evolution of N_2O (g) emissions. Two application/irrigation events occurred at day 0 and day 15, respectively, indicated by downward arrows.

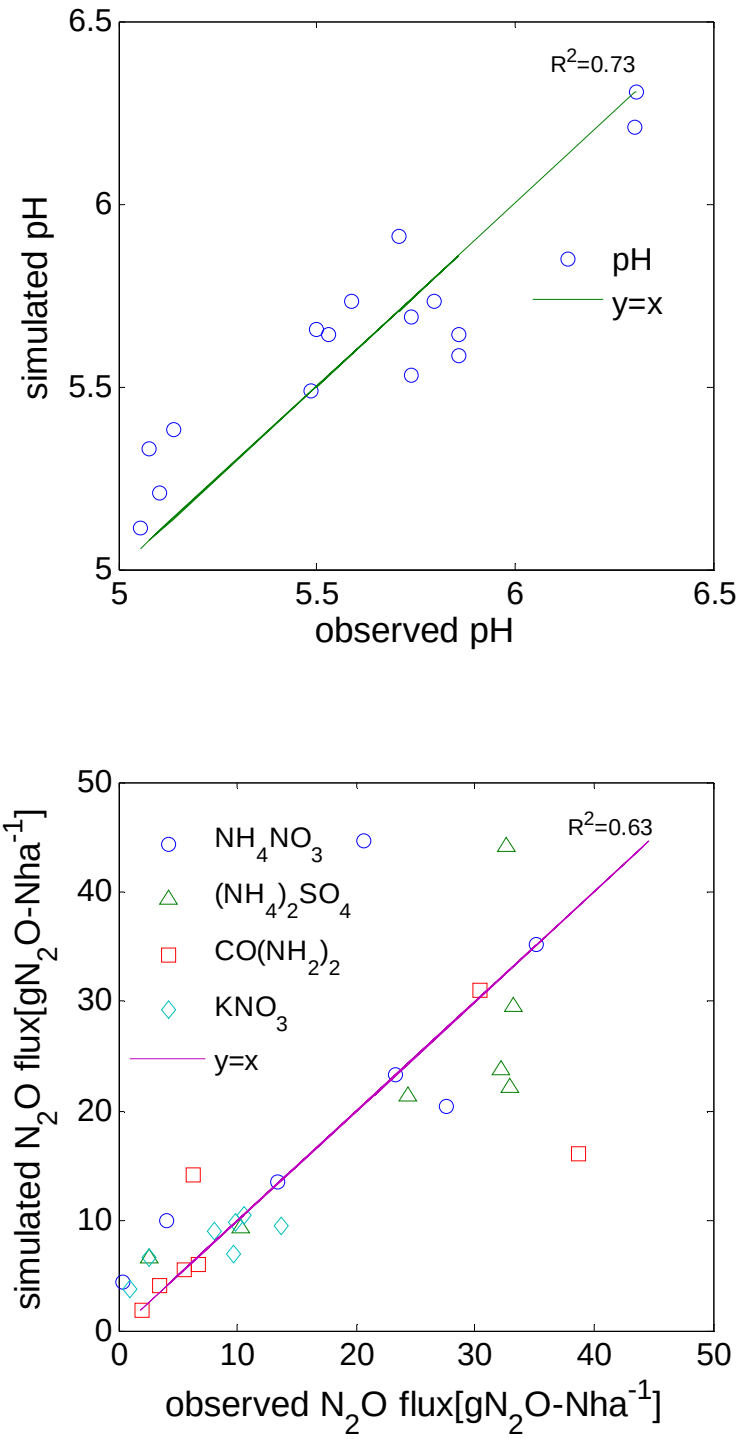

Figure 5 The observed vs. simulated A) pH and B) N_2O flux

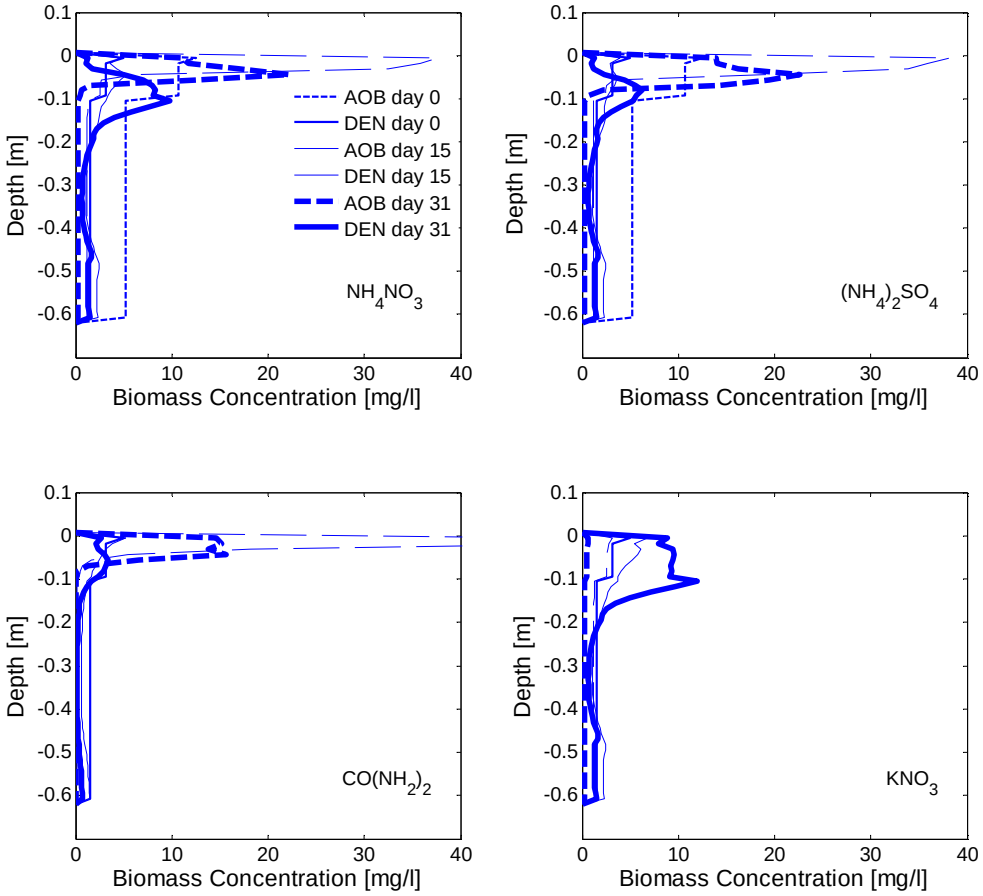

Figure 6. Predicted vertical distribution of Ammonium Oxidizer Bacteria (AOB) and Denitrifier (DEN) over time. AOB and DEN dynamics reflected the interaction with N transport in space and transformation in time.

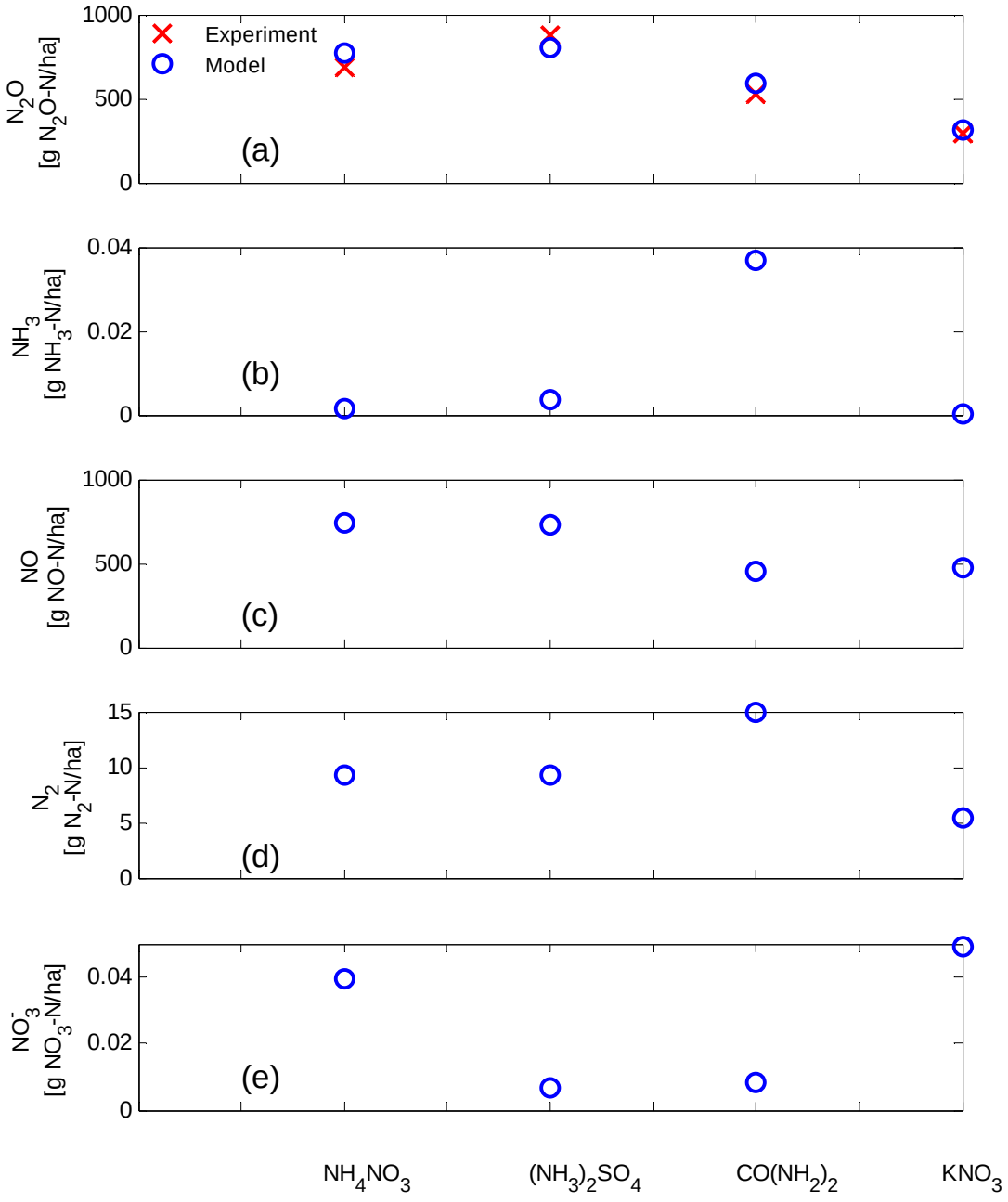

Figure 1. Time cumulative (a) N_2O, (b) NH_3, (c) NO, and (d) N_2 gases emissions and (e) NO_3^- leachate fluxes at 20 cm depth as a function of fertilizer types.

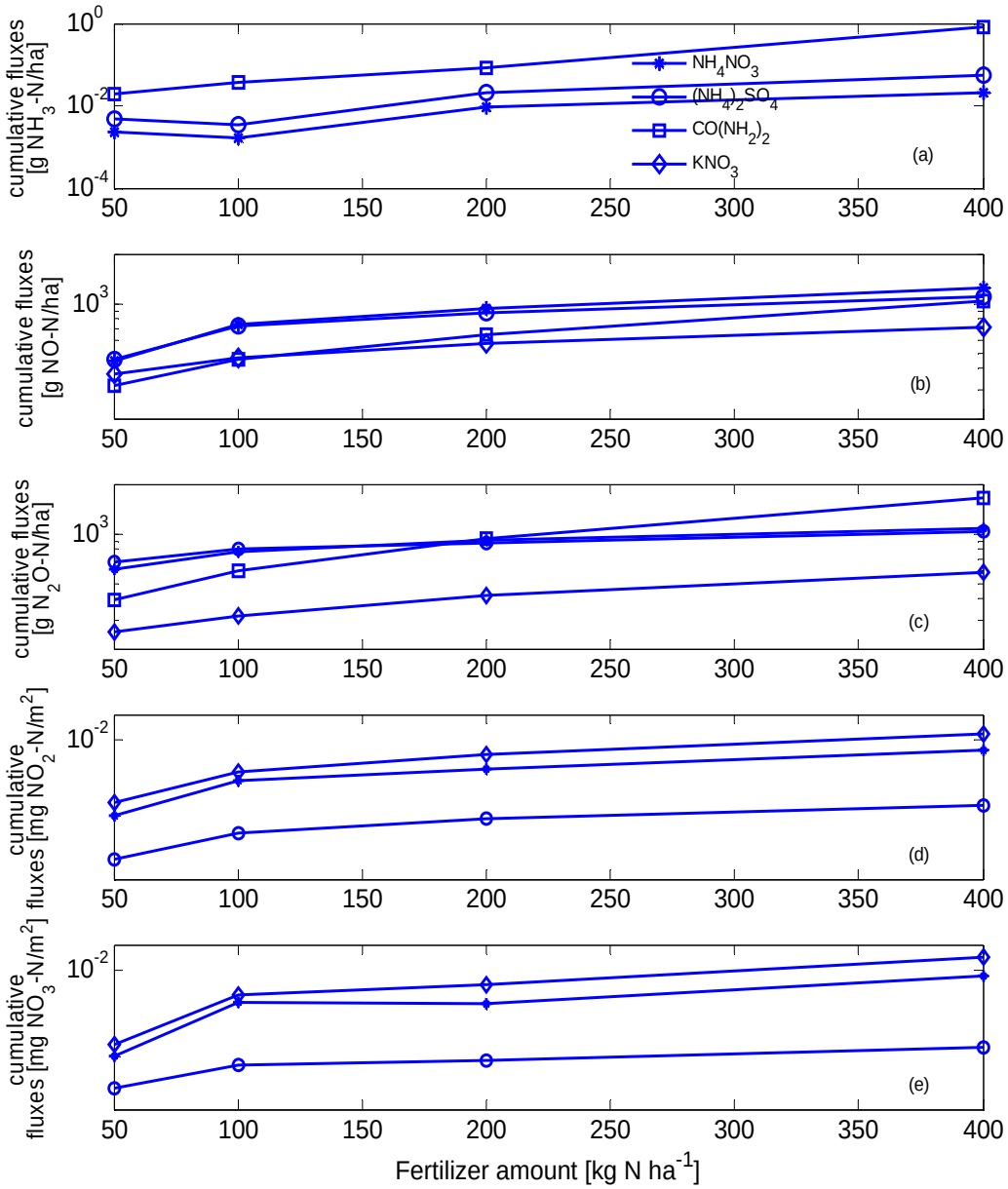

Figure 2. Time cumulative (a) NH_3, (b) NO, and (c) N_2O surface fluxes to the atmosphere, and (d) NO_2^- and (e) NO_3^- leachate fluxes at 20 cm for the four fertilizer types as functions of fertilizer amount. The NH_3 volatilization from KNO_3 and the leachate fluxes from $CO(NH_2)_2$ were negligible and thus omitted. The reference case is 100 kg N ha^{-1}. The figure is shown with a semi-log scale to illustrate the differences changes by detecting divergence or convergence of curves.

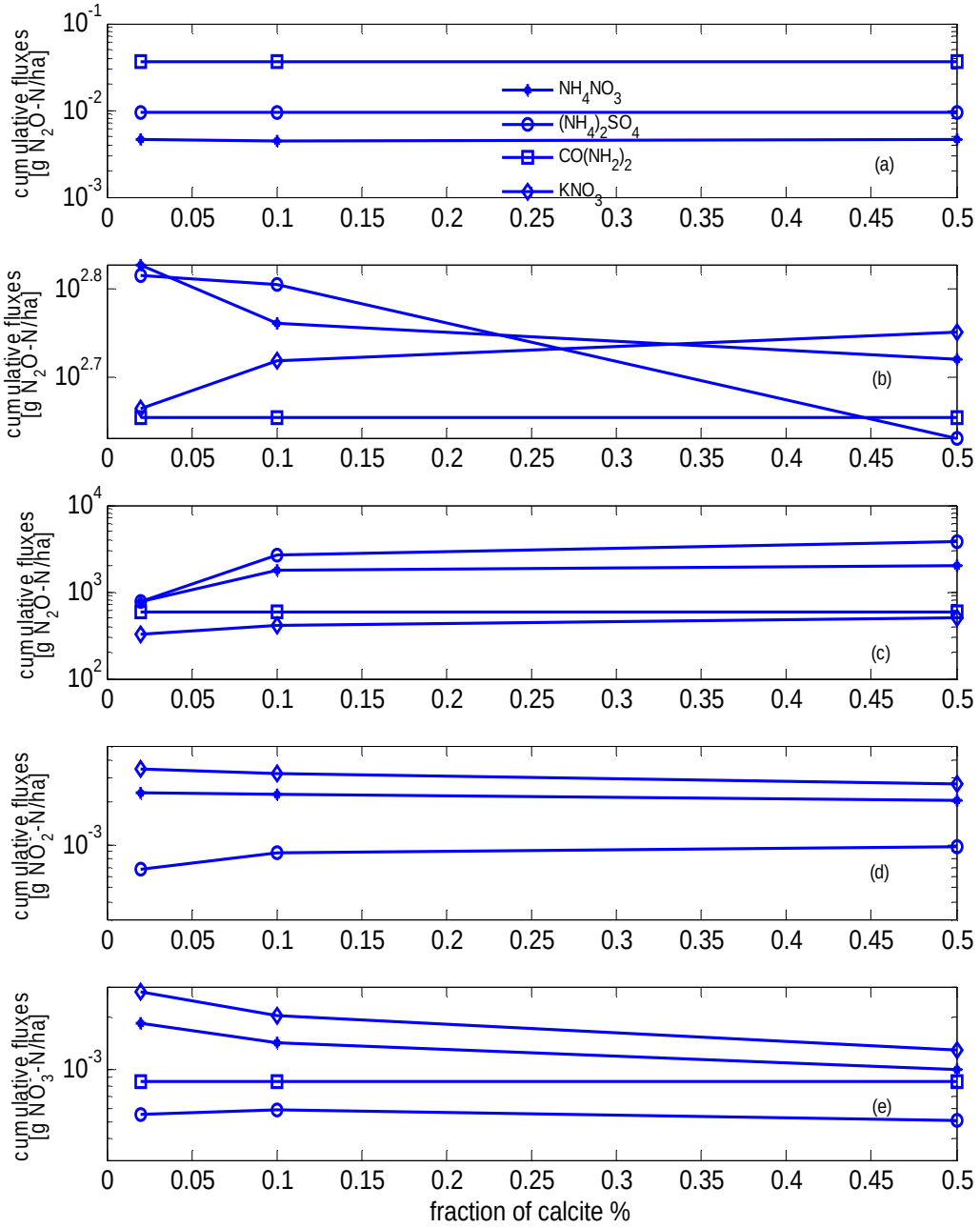

Figure 9. Time cumulative (a) NH_3, (b) NO, and (c) N_2O surface fluxes to the atmosphere, and (d) NO_2^- and (e) NO_3^- leachate fluxes a3

t depth of 20 cm for the four fertilizer types as functions of soil calcite fraction. The NH_3 volatilization from KNO_3 and the leachate fluxes from $CO(NH_2)_2$ were negligible and thus omitted.

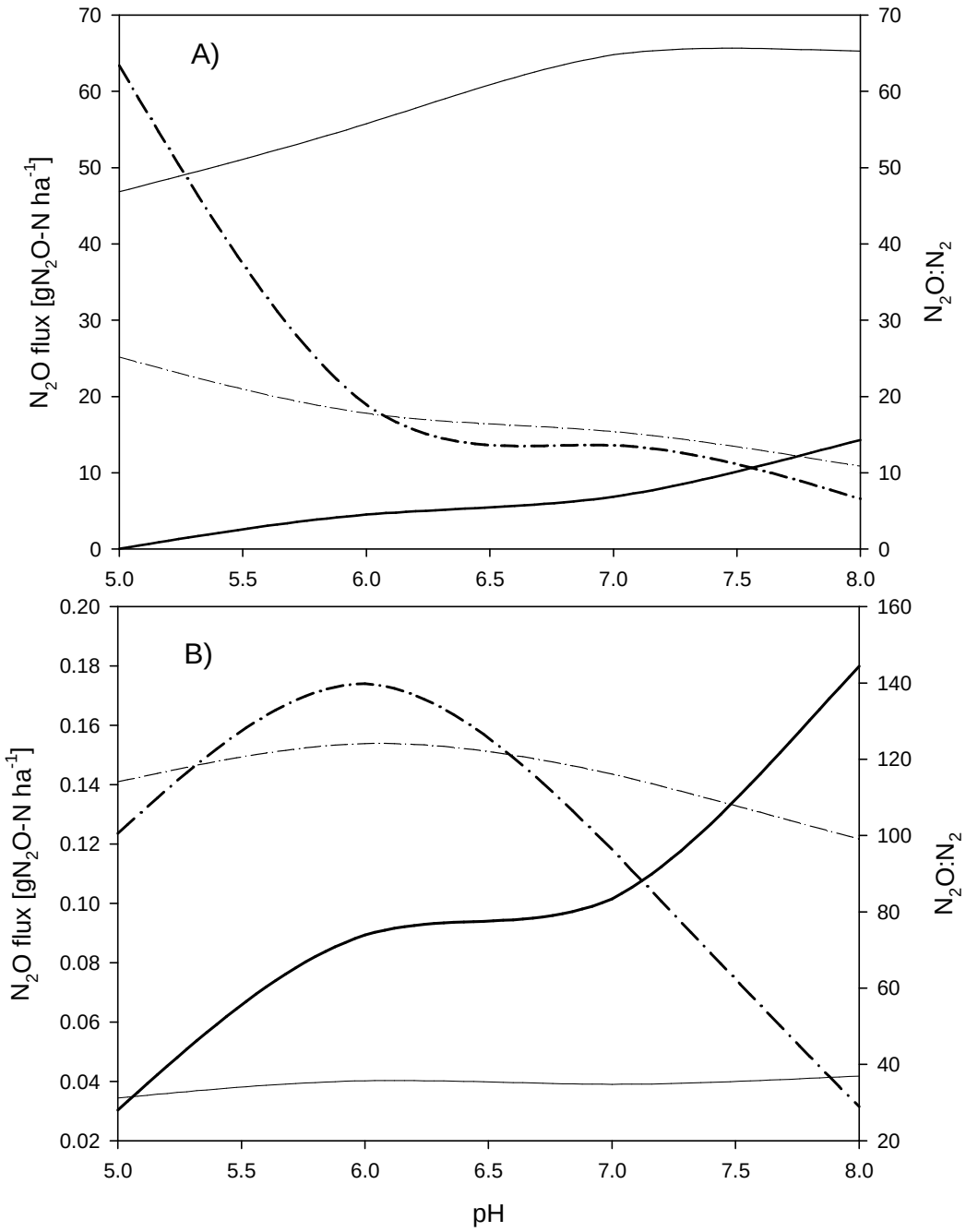

Figure 10 Predicted N_2O emissions and N_2O/N_2 ratio from NO_3^- or NH_4^+ treatments as a function of soil pH. Solid lines indicate N_2O flux and dash lines indicate N_2O/N_2 ratio. Thick lines indicate NH_4^+ treatment and thin lines indicate NO_3^- treatment. The figures shown correspond to two soils: A) clay loam and B) sandy loam